[4] R. L. Shubkin, *Synthetic Lubricants and High-Performance Functional Fluids* (Ed.: R. L. Shubkin), Marcel Dekker, New York, **1993**, pp. 1 – 40.
[5] C. T. O'Connor, M. Kojima, *Catal. Today* **1990**, *6*, 329 – 349.
[6] V. N. Ipatieff, B. B. Corson, G. Egloff, *Ind. Eng. Chem.* **1935**, *27*, 1077 – 1081.
[7] S. A. Tabak, F. J. Krambeck, W. E. Garwood, *AIChE J.* **1986**, *32*, 1526 – 1531.
[8] K. G. Wilshier, P. Smart, R. Western, T. Mole, T. Behrsing, *Appl. Catal.* **1987**, *31*, 339 – 359.
[9] J. P. van den Berg, J. P. Wolthuizen, A. D. H. Clague, G. R. Hays, R. Huis, J. H. C. van Hooff, *J. Catal.* **1983**, *80*, 130 – 138.
[10] C. S. H. Chen, R. F. Bridger, *J. Catal.* **1996**, *161*, 687 – 693.
[11] R. J. Quann, L. A. Green, S. A. Tabak, F. J. Krambeck, *Ind. Eng. Chem. Res.* **1988**, *27*, 565 – 570.
[12] C. Naccache, *Deactivation and Poisoning of Catalysts*, *Chemical Industries Series Vol. 20*, Marcel Dekker, New York, **1985**, pp. 185 – 203.
[13] W. M. Meier, D. H. Olson, C. Baerlocher, *Zeolites* **1996**, *17*, 1 – 230.
[14] S. Ernst, J. Weitkamp, *Stud. Surf. Sci. Catal.* **1991**, *65*, 645 – 652.
[15] J. L. Schlenker, J. B. Higgins, E. W. Valyocsik, *Zeolites* **1990**, *10*, 293 – 296.
[16] E. W. Valyocsik, N. M. Page, *Eur. Pat. Appl.* 174121, **1986**.
[17] S. D. Picket, A. K. Nowak, J. M. Thomas, A. K. Cheetham, *Zeolites* **1989**, *9*, 123 – 135.

Tribochemical Activation of Iron Oxide for the Reduction of NO with CO: How Lattice Defects Can Influence the Catalytic Activity

Thomas Rühle, Olaf Timpe, Norbert Pfänder und Robert Schlögl*

The cleavage of NO_x molecule into its constituent elements is an important goal for environmental catalysis.[1] Massive metal oxides are, in principle, a suitable class of compounds[2] and have been discussed for a long time as potential catalysts,[3] however had neither the required activity nor stability against reduction.

Iron oxide is non-toxic and chemisorbs NO very well[4] and is thus a promising material, provided that the active centers can be regenerated by a reducing agent such as CO.[5] Iron oxide nano particles are currently the subject of extensive investigations in NO reduction processes.[6] nonstationary kinetic measurements[7] show that in hematite (α-Fe_2O_3) NO is absorbed and activated at defects in the oxygen sublattice.[8] Conversion into N_2 proceeds via the intermediate N_2O. The active sites are regenerated by the reaction of CO with oxygen. In comparison to other catalysts iron oxide exhibits a high selectivity for N_2, but not for N_2O,[6, 9] an important feature for application in environmental catalysis.

When the reaction with CO is not limited to the surface active sites then the catalysts is rapidly following the chemistry of the blast-furnace reduction of iron oxide. This reaction pathway requires the diffusion of iron out of the bulk material and onto the surface.[10] Thus it is necessary to maximize the number on active sites but at the same time the bulk diffusion of the iron atoms has to be controlled.

The tribochemical (that is, induced through high-energy ball milling) activation of commercial hematite leads to a clear improvement in the catalytic properties of the material. The conversion – temperature profile (Figure 1) shows a considerable increase in catalytic activity after the grinding process. At the temperature at which the unactivated oxide begins to react the activated sample shows its greatest activity. Compared to supported oxide particles[7] that give active catalysts with an internal surface of 302 $m^2 g^{-1}$ the catalyst presented herein, which has an internal surface of only 8.2 $m^2 g^{-1}$, is significantly more active, as can be seen by comparing the measured values at 50 % conversion (here 482 K, supported sample 578 K) and at 80 % conversion (here 532 K, supported sample 615 K). The comparison of the almost identical NO conversion and CO_2 yield curves in Figure 1 demonstrates clearly the excellent selectivity[11] of the catalyst to N_2, that is achieved here even without a high surface-area activated charcoal support and the addition of promoter oxides.[12] This result also demonstrates the high stability of the ground iron oxide against irreversible reduction.

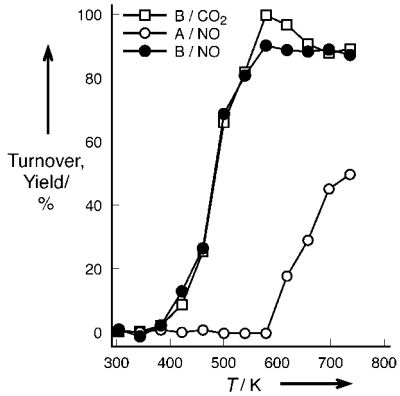

Figure 1. Conversion – temperature profile of the NO – CO reaction on pure unactivated (A) and activated iron oxide (B) (For B/CO_2 it is not the conversion but the yield curve). After activation the Brunauer – Emmett – Teller (BET) surface is not measurably different from the starting value. The modified residence time[7] was in each case 100 kg s mol^{-1}.

The effect of the tribochemical treatment on the activity was emphasized by comparing the activation energies of the NO reduction by iron oxide and by a highly dispersed platinum catalyst[13]. Figure 2 shows the Arrhenius plot of the corresponding data from stationary measurements. The activation improves the specific activity of the iron oxide compared to that of the supported platinum metal. Moreover, the apparent activation energy of the reaction on the iron oxide reduces from 82 to 45 kJ mol^{-1} and is thus comparable to that of the platinum catalyst (50 kJ mol^{-1}; a value that compares well with literature data[14]). This observation is noteworthy because the mechanism of the reactions on platinum and iron ought to be different.[15]

[*] Prof. Dr. R. Schlögl, Dipl.-Chem. T. Rühle, Dr. O. Timpe, N. Pfänder
Fritz-Haber-Institut der Max-Planck Gesellschaft
Faradayweg 4 – 6, 14195 Berlin (Germany)
Fax: (+49) 30-8413-4401
E-mail: andrea@fhi-berlin.mpg.de

  1433-7851/00/3923-4379 $ 17.50+.50/0

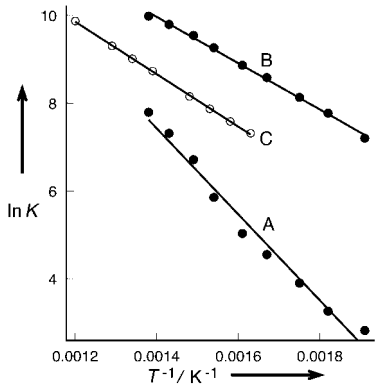

Figure 2. Determination of the apparent activation energy from the NO conversion; A) unactivated iron oxide, B) platinum on aluminum oxide, C) activated iron oxide. The errors are about twice as large as the data symbols for sample A.

The catalytic activity remained constant for 30 hours, during which the concentrations of the reaction gases and the temperature were changed many times in a steps-wise manner. This confirms the excellent stability of the active sites up to a maximum temperature of 773 K. Thermal pretreatment up to 873 K did not have a negative effect on the catalytic behavior.

The chemical stability after activation was tested through pulse treatment under reducing conditions. Figure 3 shows pulse responses to CO (5% in He carrier gas) at 673 K. After

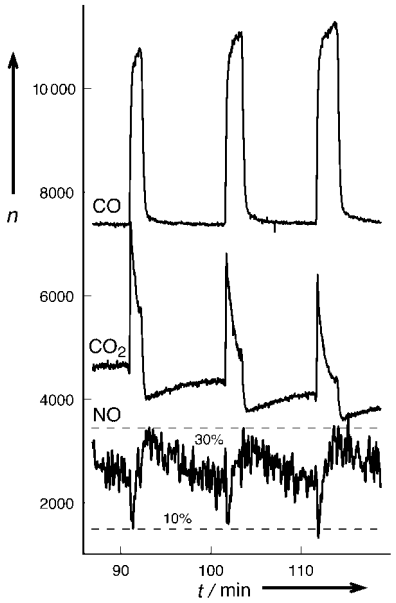

Figure 3. Pulse responses of an activated catalyst to the addition of CO (5% in He carrier gas) to the reaction gas mixture; n = IMR mass spectrometer count rate [events per second].

a very short period of improved NO conversion the SCR activity (SCR = selective catalytic reduction) reduces by 70% conversion, then after the end of the reductive pulse, slowly recovers to the initial value. The regeneration process, which has a time span of around 5 min, is assigned to the reoxidation of the iron (2+) centers in the bulk material; these result from a fast reaction under the influence of CO, as the CO_2 pulse responses in Figure 2 suggest. The unactivated sample is completely and irreversibly deactivated by a single one of these CO pulses

The stability of the activated catalysis to gaseous oxygen is an important point as the defects near to the surface of the oxygen lattice in hematite seem to be responsible for the catalytic properties. Figure 4 reveals that the selectivity of the

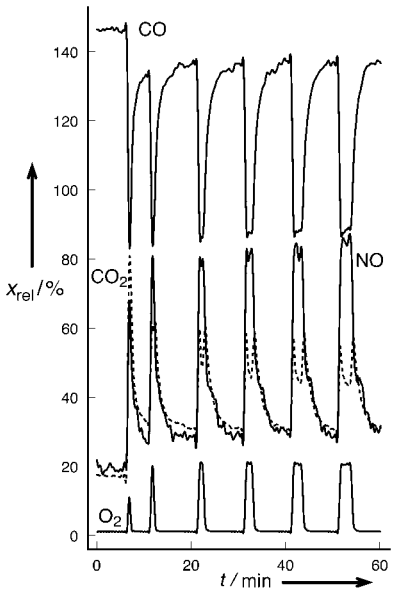

Figure 4. Pulse response of an activated catalyst to the addition of O_2 (2% in He carrier gas) to the reaction gas mixture. The pulse response in the CO_2 channel is shown as a broken line; x_{rel} = relative amount [%].

SCR reaction in the presence of oxygen (2% in He) is significantly diminished, however, rapidly recovers. The pulse profiles for CO and CO_2 are clearly not mirror images of one another which indicates that, in addition to the expected competition between the SCR reaction and the total oxidation of CO, other processes must also be occurring. After longer exposure to oxygen the conversion of CO_2 shows a transient effect that is distinguished by the combustion of carbon which does not come directly from the gas phase. Apparently the catalyst is able to store CO when the catalyst surface is transformed into a particular oxidation state that is higher than that under stationary opperation.[16] In response to the composition of the gas phase the surface of the iron oxide changes its composition[17] and thus, its coverage of CO and NO. As a result of this behavior we observe a change in the selectivity of the SCR reaction and a CO storage effect.

The catalytic behavior demonstrates that the tribochemical activation leads to considerable disorder in the oxygen lattice at the surface, but without the occurrence of irreversible deactivation by reduction. The limitation of the catalytic activity by diffusion processes in the oxygen lattice was confirmed by modeling the nonstationary kinetic measurements for N_2O reduction on a supported iron oxide sample.[18] The resulting activation energy for oxygen diffusion (47 kJ mol^{-1}) corresponds very well to the value determined here for the activated sample.[19]

  1433-7851/00/3923-4380 $ 17.50+.50/0 *Angew. Chem. Int. Ed.* **2000**, *39*, No. 23

A significant change in the internal structure of the hematite was demonstrated by means of transmission electron microscopy (TEM). Figure 5A shows at the edge of an oxide particle a nano particle (green) that has been formed by the grinding process and that is surrounded by an amorphous layer which also forms the outer surface of the particle. The internal structure of the polycrystalline particle[20] is highly disrupted (Figure 5B and C). It seems plausible that the amorphous regions (green in Figure 5B, blue in Figure 5C) and breaks in the (104) crystal plane (green in Figure 5C) hinder the migration of the iron ions in the bulk material. Under the present reaction conditions this migration controls the reduction to iron.[21]. Figure 5D displays the intact structure of starting material prior to grinding, which is free from an amorphous covering layer (red in Figure 5D). The diffraction pattern of the activated hematite (Figure 5E) does not show any foreign-phase reflections and indicates that disrupted crystalline regions (large dotlike reflections) and highly amorphous substance (ring structure) lie next to each other. The X-ray powder diffraction diagram[22] also does not show a foreign phase but indicates the loss of around 90% of the scattering power of the sample after activation.

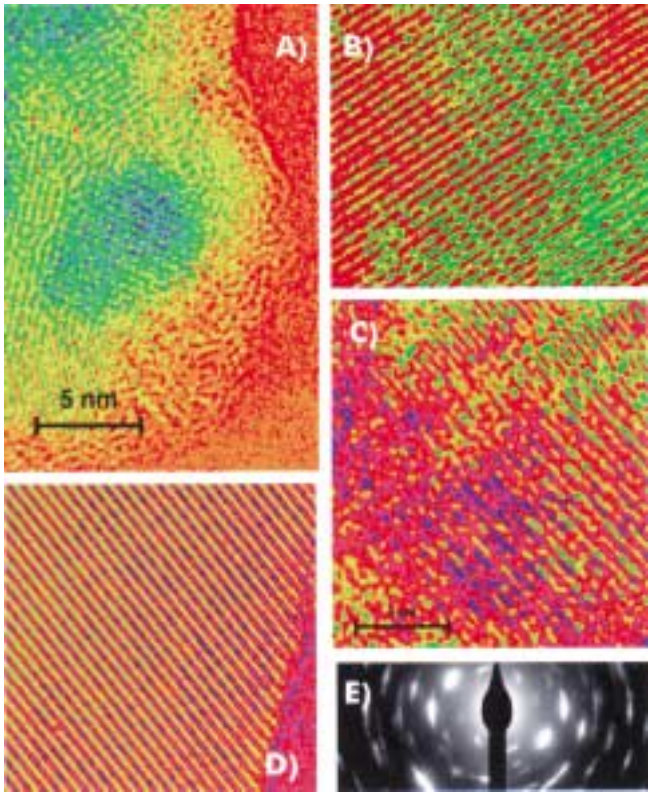

Figure 5. TEM image (Philips CM200FEG, 200 kV, samples dispersed by ultrasound in CCl_4, measured on charcoal) of an activated catalyst (images A–C, E) and the untreated material (image D). In images A–C the (104) crystal planes with an average separation of 0.27 nm and in image D the (012) crystal planes with a separation of 0.37 nm can be seen. The crossed lattice planes in the oxide cluster (green) in image A correspond to the (024) crystal plane with a separation of 0.18 nm.

The inhibition of the migration of iron ions by tribochemical activation up to "the grinding equilibrium"[23] was confirmed by temperature programmed reduction (TPR) in a hydrogen atmosphere. From the integrated mass loss[24] the contribution of vacant oxygen sites[25] was determined to be 1.8 mass %. The profile of the two-step reaction[26] from hematite to magnetite (Fe_3O_4) and then to iron has a relative hydrogen consumption of 1:9 which indicates the phase purity of the activated sample. The profile of the reduction of the ground material indicates two double structures which intergrate in the ratio of 10:90, the first of which (at 584 and 724 K) can be assigned to the reduction of the crystalline hematite and the second (at 640 and 803 K) corresponds to a kinetically delayed reduction reaction. The quantitative agreement of this analysis with the loss of scattering power in the X-ray powder diffraction shows that around 90% of the mass of the hematite becomes amorphous and thus kinetically hinders the reduction.

Through variation of the heating rate in the TPR[27] and a deconvolution corresponding to the two differently damaged lattice sections of hematite it was determined that only the formation of magnetite from hematite[28] is kinetically hindered while the subsequent reaction to metallic iron is in fact significantly easier after activation.[29]

The results show that it is possible to increase the number of defects in the oxygen lattice that are necessary for catalysis and at the same time to increase the kinetic stability of the activated iron oxide in the form of hematite.[30] This apparent contradiction to chemical intuition[31] can be explained in that the metal-oxide reduction is at least a two-step process and the rate-limiting steps (the reorganization of the iron lattice for the formation of the magnetite and the oxygen migration for the formation of iron) are dependent in different ways upon the induced lattice defects. This example shows further that the controlled change of the bulk structure of a material really can cause significant improvements in catalytic activity and stability without the need to alter the usual „design variables" of heterogeneous catalysis, the chemical composition and the particle size.

Experimental Section

Hematite (Fluka, 99.5% pure) was activated in a Retsch-Kugelmühle S2 in a steel grinding vessel. Dry grinding gave the grinding equilibrium after 45 h (first 24 h with 50 $kg\,m\,s^{-2}$ and then 21 h with 100 $kg\,m\,s^{-2}$). The determination of the metallic impurities by X-ray fluorescence analysis before/after the activation gave the following values: Cu: 1130/1190; Cr: 1640/2000; Ni: 140/400 ppm. Photoelectron spectroscopy (XPS) could not detect the presence of any of the impurities in the surface of the sample.

The activity measurements were carried out in quartz-glass flow reactor (blind activity with SiC substitute filling: 4% conversion of NO at 723 K) using 20 mg of activated sample. A flow of dry helium (100 $mL\,min^{-1}$), that contained NO (1700 ppm) and CO (10000 ppm), was employed as the reaction gas mixture. Detection was with an ATOMIKA 1500 IMR mass spectrometer (IMR = ion molecule reaction), which with the use of the primary gasses Kr, Xe, and CF_3I could analyze quantitatively the gas components NO, CO, NO_2, CO_2 without cross sensitivity. The amount of N_2 was determined partially quantitatively through electron impact ionization mass spectrometry. For the IMR mass spectroscopic quantification relative sensitivity factors of 1:100:600 for NO:CO:CO_2 were used. For calibration benzene was used as an internal standard.

Received: May 9, 2000 [Z15104]

  1433-7851/00/3923-4381 $ 17.50+.50/0

[1] R. M. Heck, *Catal. Today* **1999**, *53*, 519 – 523.
[2] G. Mul, W. D. Zhu, F. Kapteijn, J. A. Moulijn, *Appl. Catal. B* **1998**, *17*, 205 – 220.
[3] M. Shelef, *Chem. Rev. Sci. Eng.* **1975**, 1 – 40; S. Okazaki, H. Kuroha, T. Okuyama, *Chem. Lett.* **1985**, 45.
[4] G. V. Glazneva, A. A. Davidov, I. S. Sazunova, Y. M. Shchekochikin, N. P. Keier, *React. Kin. Catal. Lett.* **1978**, *9*, 131 – 136; A. Zecchina, F. Geobaldo, C. Lamberti, S. Bordiga, G. T. Palomino, C. O. Arean, *Catal. Lett.* **1996**, *42*, 25 – 33; J. P. Contour, G. Mouvier, *J. Catal.* **1975**, *40*, 342 – 348.
[5] A. N. Hayhurst, A. D. Lawrence, *Combust. Flame* **1997**, *110*, 351 – 365.
[6] G. Centi, F. Vazzana, *Catal. Today* **1999**, *53*, 683 – 693; X. Feng, W. K. Hall, *Catal. Lett.* **1996**, *41*, 45; H. Y. Chen, W. M. H. Sachtler, *Catal. Today* **1998**, *42*, 15; R. Q. Long, R. T. Yang, *J. Catal.* **1999**, *186*, 254 – 268.
[7] H. Randall, R. Doepper, A. Renken, *Can. J. Chem. Eng.* **1996**, *74*, 586 – 594.
[8] K. Otto, M. Shelef, *J. Catal.* **1970**, *18*, 184.
[9] F. Nakajima, *Catal. Today* **1991**, *10*, 1.
[10] W. M. Husslage, T. Bakker, M. E. Kock, R. H. Heerema, *Miner. Metall. Process.* **1999**, *16*, 23 – 33.
[11] The heterogeneously catalyzed side reaction of NO with CO to give NO_2 and carbon could be ruled out because of the absence of NO_2 in the gas phase.
[12] K. Jurczyk, R. S. Drago, *Appl. Catal. A* **1998**, *173*, 145 – 151.
[13] T. Rühle, H. Schneider, J. Find, D. Herein, N. Pfänder, U. Wild, R. Schlögl, D. Nachtigall, S. Arelt, U. Heinrich, *Appl. Catal. B* **1997**, *14*, 69 – 84.
[14] P. Lööf, B. Kasemo, S. Anderson, A. Frestadt, *J. Catal.* **1991**, *130*, 181.
[15] K. C. Taylor, *Catal. Rev. Sci. Eng*. **1993**, *35*, 457 – 481; Th. Fink, J. P. Dath, M. R. Bassett, G. Ertl, *Surf. Sci*. **1991**, *245*, 96.
[16] H. Randall, R. Doepper, A. Renken, *Appl. Catal. B* **1998**, *17*, 357 – 369.
[17] X. G. Wang, W. Weiss, Sh. Shaikhutdinov, M. Ritter, M. Petersen, F. Wagner, R. Schlögl, M. Scheffler, *Phys. Rev. Lett.* **1998**, *81*, 1038 – 1041.
[18] H. Randall, R. Doepper, A. Renken, *Catal. Today* **1997**, *38*, 13 – 22.
[19] It is assumed that the processes of iron oxide reduction by CO and its reoxidation by nitrogen oxide are spatially and temporally decoupled. The "regenerative reaction path", by which the oxygen is transported from the site where the NO dissociates (formation of active site) to the site where CO is oxidized (consumption of active site), is different to the reaction pathway in which the coadsorbed starting materials (as on platinum[15]) react together, but corresponds to the situation supposed for partial oxidation, see: A. Bielanski, J. Haber, *Oxygen in Catalysis*, Marcel Dekker, New York, **1991**, p. 258.
[20] Through scanning electron microscopy (Hitachi-S-4000-FEG instrument, 2 kV accelerating potential) and histogram analysis over each of 500 observations the average size of the secondary particle (agglomerate) was determined. With a similar size distribution they had average values of 3 μm before and 4.2 μm after the grinding process.
[21] C. Gleitzer, *Solid State Ionics* **1990**, *38*, 133 – 141.
[22] STOE-Stadi-P instrument, $Cu_{K\alpha}$ radiation with a secondary monochromator, measurement in transmission geometry. The diffraction pattern corresponds to the ICPD-data (33-664; ICPD = international collection of powder diffraction data). By means of a Williamson – Hall analysis an increase in the stress contribution from 0.005 % in the starting material to 0.251 % in the activated material was determined. This stress was only reduced by around 50 % in thermal-healing experiments upto 873 K. The internal stress represents, in this case with an unchanged particle size and the same BET surface, the only store for the mechanically introduced energy. The activation increases the internal energy of the oxide by 933 $J\,mol^{-1}$ (determined by differential calorimetry (DSC)). See also: F. Agullo-Lopez, C. R. A. Catlow, P. D. Townsend, *Point Defects in Materials*, Academic Press, New York, **1988**; *Festkörperchemie-Beiträge aus Forschung und Praxis* (Eds.: V. Boldyrev, K. Meyer), VEB Verlag für Grundstoffindustrie, Leipzig, **1973**.
[23] R. Schrader, D. Weigelt, *Z. Anorg. Allg. Chem.* **1970**, *372*, 228.
[24] Calculated from the oxygen losses: 30.06 %; experimentally determined: 30.08 % (starting material), 29.53 % (activated material).
[25] E. E. Unmuth, L. H. Schwartz, J. B. Butt, *J. Catal.* **1980**, *61*, 242.
[26] M. M. Al-Kahatany, Y. K. Rao, *Ironmaking Steelmaking* **1977**, *7*, 149.
[27] Seiko-TG/DTA 320 instrument, sample (0.1 – 4.0 mg), heating rate varied from 0.2 to 20 $K\,min^{-1}$, reaction gas H_2 (5 %) in N_2 (flow rate 80 $mL\,min^{-1}$); water, the reaction product, was detected on-line with IMR mass spectrometry in conjunction with thermogravimetry(TG)/differential thermogravimetry(DTG)/differential thermoanalysis-(DTA) signals.
[28] Values for the not ground, and for the X-ray crystalline sections in the ground samples 63 $kJ\,mol^{-1}$ and in the X-ray amorphous sections 87 $kJ\,mol^{-1}$.
[29] The lower activation energy (132 $kJ\,mol^{-1}$ for the not ground and X-ray crystalline parts, 90 $kJ\,mol^{-1}$ for the amorphous) contradicts the observed increased maximum conversion-rate temperature (TPR maximum). The partial pressure of water rises following the increased reaction rate of the oxide which in turn exerts an enormous kinetic inhibition to the formation of iron. See: A. Baranski, A. Kotarba, J. M. Lagan, A. Patteck-Janczyk, E. Pyrczak, A. Reizer, *Appl. Catal. A* **1994**, *112*, 13 – 36.
[30] G. Näser, W. Scholz, *Kolloid Z.* **1958**, *156*, 1
[31] C. Politis, *Z. Phys. Chem. (Munich)* **1988**, *157*, 208 – 220; "Ammonia synthesis": R. Schlögl, in *Handbook of Heterogeneous Catalysis* (Eds.: G. Ertl, H. Knözinger, J. Weitkamp), VCH, Weinheim, **1995**, pp. 1698 – 1747.

  1433-7851/00/3923-4382 $ 17.50+.50/0